INTERNATIONAL JOURNAL OF
ENERGY AND ENVIRONMENT

Volume 2, Issue 4, 2011 pp.627-640
Journal homepage: www.IJEE.IEEFoundation.org

Performance characteristic of energy selective electron (ESE) heat engine with filter heat conduction

Zemin Ding, Lingen Chen, Fengrui Sun

College of Naval Architecture and Power, Naval University of Engineering, Wuhan 430033, P. R. China.

Abstract
The model of an energy selective electron (ESE) heat engine with filter heat conduction via phonons is presented in this paper. The general expressions for power output and efficiency of the ESE heat engine are derived for the maximum power operation regime and the intermediate operation regime, respectively. The optimum performance and the optimal operation regions in the two different operation regimes of the ESE heat engine are analyzed by detailed numerical calculations. The influences of filter heat conduction and the temperature of hot reservoir on the optimum performance of the ESE heat engine are analyzed in detail. Furthermore, the influence of resonance width on the performance of the ESE heat engine in intermediate operation regime is also discussed. The results obtained herein have theoretical significance for understanding and improving the performance of practical electron energy conversion systems.

Keywords: Energy selective electron (ESE) heat engine; Filter heat conduction; Power and efficiency characteristic.

1. Introduction

Recently, the study of energy conversion systems in microscopic scale is attracting considerable interests. Typical examples of these systems include thermionic power generators and refrigerators [1-11], Brownian motors [12-23], quantum ratchet [24-29], and so on. For the thermionic energy conversion systems, heat transfer is achieved by removing high energy electrons from one reservoir to the other, and all the devices use barriers or other energy selection mechanisms such as resonant tunneling to limit the current flowing in the device to electrons in particular energy ranges [1-3, 30]. While Brownian motors usually use the temperature differential [31, 32] as the source of non-equilibrium to power a ratchet, which combines asymmetry with nonequilibrium process to generate directed motion of Brownian particles. In a quantum ratchet, the classical Brownian particles in the rocked ratchet are replaced by quantum particles, which have the ability to tunnel through narrow barriers and to be wave-reflected from sharp barriers. Comparing the quantum ratchet with the classical ratchet, it can be found that not only the height of a potential barrier but also the shapes of the ratchet potential have been changed in the quantum ratchet system. Reimann *et al*. [24] theoretically predicted the existence of the temperature dependent net current reversal for quantum particles in a rocked ratchet, and it was observed in the experiment by Linke *et al*. [25] for electrons in ballistic transport regime. Yukawa *et al*. [26] proposed two models of quantum ratchet and studied the finite net flow produced in them. Khrapai *et al*. [27, 28] studied the quantum ratchet phenomenon of quantum point contacts. Hoffmann and Linke [29] found that a two-terminal quantum dot bridging a temperature difference could operate as a thermometer by probing the Fermi-Dirac distributions of the electron gas on both sides of the quantum dot and discussed the three different operation regimes of the device.

Based on the experimental work [25, 33-35] on quantum ratchet, Humphrey *et al*. [36] and Linke *et al*. [37-38] studied the performance of quantum ratchet acting as a heat pump. Humphrey *et al*. [39] further proposed a novel mechanism of quantum Brownian heat engine model for electrons. This mechanism combines the energy selective property of electrons in thermoelectric and thermionic systems with the temperature differential driving property of Brownian heat engine, and it is termed as the energy selection electron (ESE) heat engine [40]. The ESE heat engine utilizes a temperature difference between two electron reservoirs to transport high energy electrons against an electrochemical potential gradient. The electrons are transported between the two reservoirs through an energy filter, which freely transmits electrons in a specified energy range and blocks the transport of all others. Such an energy filter could be realized by the resonance in a quantum dot [39, 41] or a superlattice [42, 43]. It was shown that the ESE heat engine could operate at Carnot efficiency when the energy of the filter was suited at which the Fermi distributions in the two reservoirs had the same value [39]. This was called the reversible operation regime of operation of the ESE heat engine.

Such an energy selective electron heat engine is of theoretical significance to thermionic power generators and refrigerators. Thermionic power generators and refrigerators are actually energy selective systems, for they utilize an energy barrier to selectively transmit high energy electrons ballistically between the reservoirs. Because of the lack of a kind of barrier material with sufficiently low work function [1, 2], traditional vacuum thermionic devices with macroscopic gaps between emitter and collector plates are limited to very high temperature applications ($T_H > 1000K$). Nanostructures are being investigated in an attempt to develop thermionic devices that can refrigerate or generate power at low temperature [3, 4], and successful solid-state thermionic cooling of up to a few degrees has been reported [42, 44]. The transmission of electrons in these nanostructures devices share the same way as the ESE engine system discussed in this paper. The results obtained in Refs. [39, 40] have already been applied to study the performance of thermoelectric and thermionic energy conversion systems [9-11, 45-49].

In the past few decades, there has been tremendous progress in the investigation on the performance characteristics and optimization of conventional macroscopic energy conversion systems by scientists and engineers using finite time thermodynamics [50-59]. Performance optimization and the transmission losses between the reservoirs in energy conversion systems are two major considerations in finite time thermodynamics. Recently, the theory of finite time thermodynamics has also been used to study the performance of microscopic energy conversion systems, such as Brownian ratchet [60-66], molecular motors [67], quantum ratchet [68, 69] and electron engines [40], and many new results have been obtained. Velasco *et al.* [60] and Tu [65] studied the optimal performance of the Feynman engine using the method of finite time thermodynamics. And the optimum performance of thermal Brownian motors was also investigated by some authors [61-64, 66]. Schmiedl and Seifert [67] analyzed the efficiency performance of molecular motors at maximum power condition. Esposito *et al.* [68] identified the operational conditions for maximum power of a nanothermoelectric engine consisting of a quantum dot embedded between two leads at different temperatures and chemical potentials, and found that the thermoelectric efficiency at maximum power agrees with the expression for Curzon-Ahlborn efficiency [70] up to quadratic terms. Esposito *et al.* [69] investigate the finite time thermodynamics of a single level fermion system interacting with a thermal reservoir through a tunneling junction.

As to the electron heat engine systems, Humphrey [40] analyzed the optimal performance of ESE heat engine operating at maximum power operation regime and intermediate operation condition (i.e. between maximum power operation and reversible operation), respectively. Similar to the conventional energy conversion systems, there also exist the transmission losses in the electron engine systems. In fact, the filter in the electron engine will conduct heat between the two electron reservoirs due to the propagation of phonons. This heat leak between hot and cold reservoirs should have significant influence on the performance of an electron heat engine. And results of previous researches [71-73] have shown that the heat conduction by the barrier material is of great importance for the performance of electron energy devices, such as thermoelectric and thermionic power generators and refrigerators. He *et al.* [74] studied the optimum performance of an electron refrigerator with heat leaks in the intermediate operation regime. Ding *et al.* [75] analyzed the influences of filter heat conduction on the optimum performance of the ESE refrigerator in both maximum cooling load operation regime and the intermediate operation regime.

However, results about the ESE heat engine model in Refs. [39, 40] are obtained with out considering the heat conduction of the filter due to the propagation of phonons. So far, the optimum performance of the ESE heat engine with filter heat conduction via phonons and the influence of this heat conduction on the performance of the heat engine have been rarely investigated. Thus, based on Refs.[39, 40, 74, 75], this paper takes a further step to present an ESE heat engine model with heat conduction of the energy filter via phonons, and to analyze the optimum performance of the model as well as the influence of the heat conduction of the filter. The general formula for power output and efficiency of the ESE heat engine are derived for the maximum power operation regime and the intermediate operation regime, respectively. Through numerical calculations, for the two different operation regimes, the optimum regions of power output and efficiency are obtained and the influences of heat conduction as well as the temperature of hot reservoir on the optimum performance of the device are analyzed in detail. The influence of the resonance width on the power and efficiency characteristic of the ESE heat engine at intermediate regime is also discussed.

2. Model of an ESE heat engine with filter heat conduction

The schematic diagram of an ESE heat engine with filter heat transfer is shown in Figure 1. It consists of two infinitely large electron reservoirs and an energy filter. The two reservoirs have different temperatures and chemical potentials, where T_C and T_H are the temperatures of cold and hot reservoirs, μ_C and μ_H are the chemical potentials of cold and hot reservoirs. They interact with each other only via the energy filter which freely transmits electrons with a specified range of energies. Meanwhile, the filter itself has a thermal conductivity k_f and contributes to the heat transfer between the two reservoirs. In Figure 1, E_R is the central energy of the resonance energy level in the energy filter, ΔE is the width of the resonance, eV_0 is a bias voltage that is applied to the hot reservoir.

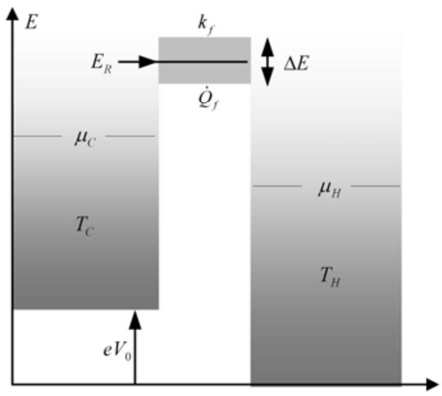

Figure 1. Schematic diagram of the ESE heat engine with filter heat conduction

According to the above description for the model, one can conclude that the heat transfer between the two reservoirs consists of two parts: one is the heat that is transferred by the electrons transmitted through the filter, and another is that transferred by the filter itself due to the propagation of phonons.

Over an infinitesimal energy range δE, the rate of released heat of the hot reservoir and the rate of absorbed heat of the cold reservoir by the transmitted electrons are [39, 40]

$$\dot{q}_{He} = \frac{2}{h}(E-\mu_H)(f_H - f_C)\delta E \tag{1}$$

$$\dot{q}_{Ce} = \frac{2}{h}(E-\mu_C)(f_H - f_C)\delta E \tag{2}$$

where h is Plank constant, and f_C and f_H are the Fermi distributions of electrons in the cold and hot reservoirs,

$$f_C = \frac{1}{1+e^{(E-\mu_C)/(k_B T_C)}} \text{ , } f_H = \frac{1}{1+e^{(E-\mu_H)/(k_B T_H)}} \tag{3}$$

where k_B is Boltzmann's constant.

While the rate of heat transferred from hot reservoir to cold reservoir by the filter itself is

$$\dot{Q}_f = k_f(T_H - T_C) \tag{4}$$

The heat conduction of the filter defined by equation (4) is similar to the bypass heat leakage of conventional heat engine provided by Bejan [76].
According to Ref. [39], the ESE heat engine could operate at Carnot efficiency when the energy of the filter is suited to $E_0 = (T_H\mu_C - T_C\mu_H)/(T_H - T_C)$, at which the Fermi distributions in the reservoirs have the same value. This is called the reversible operation regime of the ESE heat engine.

3. Performance analysis in maximum power operation regime

It was shown in Ref. [40] that, in the energy range of $E_0 < E < \infty$, electrons contribute positively to the power of the engine. So, in order to obtain the maximum power of the engine, all electrons with energies higher than E_0 should participate in the transport, while all electrons with energies below that should be blocked. This is called the maximum power operation regime of the ESE heat engine.
Thus, the rates of heat transferred by electrons at maximum power operation regime are

$$\dot{Q}_{He} = \int_{E_0}^{\infty} \dot{q}_{He} = \frac{2}{h}\int_{E_0}^{\infty} (E - \mu_H)(f_H - f_C)dE \tag{5}$$

$$\dot{Q}_{Ce} = \int_{E_0}^{\infty} \dot{q}_{Ce} = \frac{2}{h}\int_{E_0}^{\infty} (E - \mu_C)(f_H - f_C)dE \tag{6}$$

Combining equations (4)-(6) gives the total lost amount of heat of hot reservoir per unit time ($\dot{Q}_H$) and the total increased amount of heat of cold reservoir per unit time ($\dot{Q}_C$):

$$\dot{Q}_H = \dot{Q}_{He} + \dot{Q}_f \,, \dot{Q}_C = \dot{Q}_{Ce} + \dot{Q}_f \tag{7}$$

Using the first law of thermodynamics and combining equations (4)-(7), one can obtain the power and efficiency at this regime

$$P_m = \dot{Q}_H - \dot{Q}_C = -\frac{2}{h} r_0 (k_B T_H - k_B T_C)^2 \ln a \tag{8}$$

$$\eta_m = 1 - \frac{\dot{Q}_C}{\dot{Q}_H} = \frac{2r_0(k_B T_H - k_B T_C)^2 \ln a}{2(\mu_C - \mu_H)k_B T_H \ln a - k_B{}^2(T_H{}^2 - T_C{}^2)\ln^2 a - 2k_B{}^2(T_H{}^2 - T_C{}^2)g(a) - hk_f(T_H - T_C)} \tag{9}$$

where r_0, a and the function g are defined as, respectively

$$r_0 = \frac{\mu_C - \mu_H}{k_B(T_H - T_C)} \,, a = \frac{e^{r_0}}{1+e^{r_0}} \,, g(x) = \int_1^x \frac{\ln t}{1-t}dt \tag{10}$$

It can be seen from equation (8) that the power output P_m is independent of k_f and the filter heat conduction will not affect the power output P_m performance of the ESE heat engine in maximum power operation regime. To illustrate the preceding analysis, numerical examples are provided. In the calculations, it is set that $T_H = 2K$, $T_C = 1K$, $\mu_C/k_B = 12K$ and $\mu_H/k_B = 10K$.
Figure 2 shows the influence of the temperature of hot reservoir T_H on the power output P_m versus r_0 characteristic in maximum power operation regime. It can be seen that the characteristic curves of $P_m - r_0$ are parabolic like ones. There exists the optimum r_{0,P_m} which leads to the maximum power output $P_{m,max}$. The maximum power output $P_{m,max}$ increases while r_{0,P_m} doesn't change as the temperature of hot reservoir T_H increases.
Figure 3 shows the influence of the temperature of hot reservoir T_H on the efficiency η_m versus r_0 characteristic in maximum power operation regime with $k_f = 1.5\times10^{-14} W/K$. It can be seen that the characteristic curves of $\eta_m - r_0$ with filter heat conduction are parabolic like ones. There exists the optimum r_{0,η_m} which leads to the maximum efficiency $h_{m,max}$. Both the maximum efficiency $h_{m,max}$ and the optimum r_{0,η_m} will increase as the temperature of hot reservoir T_H increases.
Figure 4 shows the influence of heat conductivity k_f on the efficiency η_m versus r_0 characteristic in maximum power operation regime. It is shown that when $k_f = 0$, the efficiency in maximum power regime η_m is a monotonic increasing function of r_0 and it tends to Carnot value of $T_H/(T_H - T_C) = 0.5$ for large values of r_0, as shown by the solid line in Figure 4; when $k_f \neq 0$, the curves of $\eta_m - r_0$ are parabolic-like ones, as shown by the dashed line and dotted line in Figure 4. The maximum efficiency $h_{m,max}$ and the optimum r_{0,η_m} will decrease with the increase of heat conductivity k_f.

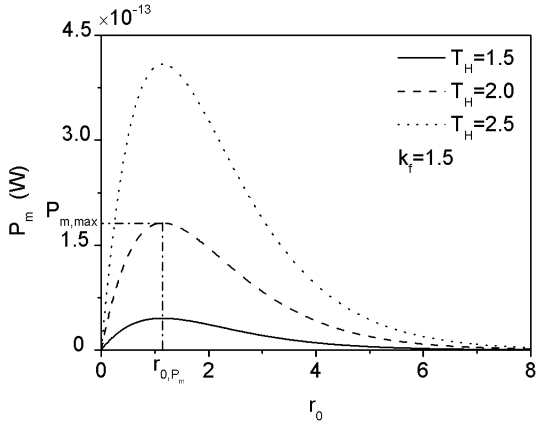

Figure 2. Influence of the temperature of hot reservoir T_H on the power output P_{m} versus r_0 characteristic in maximum power operation regime with $k_f = 1.5 \times 10^{-14} W/K$

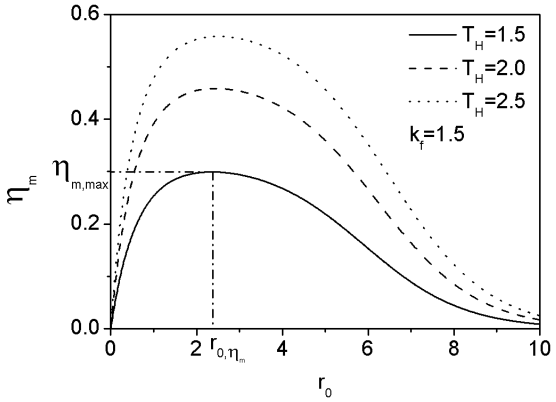

Figure 3. Influence of the temperature of hot reservoir T_H on the efficiency η_m versus r_0 characteristic in maximum power operation regime with $k_f = 1.5 \times 10^{-14} W/K$

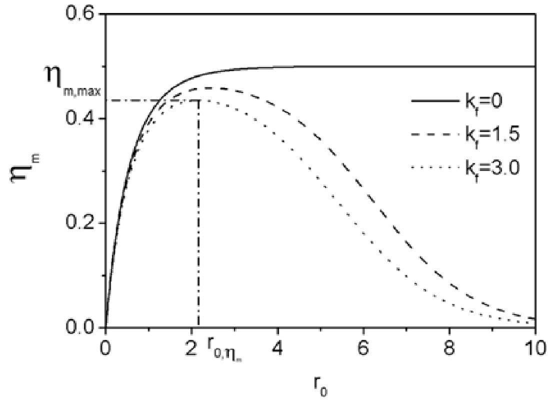

Figure 4. Influence of heat conductivity k_f on efficiency η_m versus r_0 characteristic in maximum power operation regime

Figure 5 shows the power P_m versus efficiency η_m characteristic for the ESE heat engine in maximum power regime. When there is no filter thermal conduction in the system ($k_f = 0$), the curve of $P_m - \eta_m$ is a parabolic-like one, as shown by the solid line in Figure 5. There exists an optimum efficiency which leads to the maximum power output. When the filter thermal conduction is taken into account in the system, i.e. $k_f \neq 0$, the curves of $P_m - \eta_m$ are closed loop-shaped ones, as shown by the dashed line and dotted line in Figure 5. There exist the maximum power output $P_{m,max}$ and its corresponding optimum efficiency η_{m,P_m} as well as the maximum efficiency $h_{m,max}$ and its corresponding optimum power output P_{m,h_m}.

The optimum operating regions of the ESE heat engine should be located in the regions where the $P_m - \eta_m$ curves have a negative slope. It is obvious that when the ESE heat engine operates in this region, there exist two different efficiency for a given power output. One is smaller than η_{m,P_m} and the other is larger than η_{m,P_m}. Obviously, for a given power output, one always wants to obtain the efficiency as large as possible. Thus, in the maximum power output operation regime, the optimal region of the efficiency should be

$$\eta_{m,P_m} \le \eta_m \le \eta_{m,max} \tag{11}$$

where η_{m,P_m} and $\eta_{m,max}$ are two important parameters that determine the lower and upper bounds of the optimum efficiency. The optimal operating region of the power output should be

$$P_{m,h_m} \pounds P_m \pounds P_{m,max} \tag{12}$$

where P_{m,h_m} and $P_{m,max}$ are two important parameters that determine the lower and upper bounds of the optimum power output. Moreover, the optimal region of the parameter r_0 should be

$$r_{0,P_m} \le r_0 \le r_{0,\eta_m} \tag{13}$$

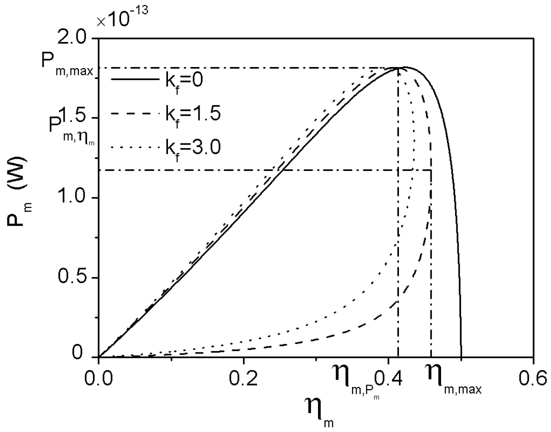

Figure 5. Influence of heat conductivity k_f on power output P_m versus efficiency h_m characteristic in maximum power operation regime

4. Performance analysis in intermediate operation regime

In intermediate operation regime, electrons with a finite energy range of ΔE around central energy E_R are transmitted through the filter. This regime can be understood to be intermediate to the reversible operation regime with maximum efficiency and the maximum power operation regime discussed above. In the system, central energy E_R is set as the primary variable. The rates of heat transferred by electrons in intermediate operation regime are [40]

$$\dot{Q}_{He} = \frac{2}{h}\int_{E_R-\Delta E/2}^{E_R+\Delta E/2} \dot{q}_{He} dE = \frac{2}{h}\int_{E_R-\Delta E/2}^{E_R+\Delta E/2} (E-\mu_H)(f_H - f_C) dE \tag{14}$$

$$\dot{Q}_{Ce} = \frac{2}{h}\int_{E_R-\Delta E/2}^{E_R+\Delta E/2} \dot{q}_{Ce} dE \frac{2}{h}\int_{E_R-\Delta E/2}^{E_R+\Delta E/2} (E-\mu_C)(f_H - f_C) dE \tag{15}$$

Combining equations (4) with (14)-(15) gives the total lost amount of heat of hot reservoir per unit time ($\dot{Q}_H$) and the total increased amount of heat of cold reservoir per unit time ($\dot{Q}_C$)

$$\dot{Q}_H = \dot{Q}_{He} + \dot{Q}_f \,, \dot{Q}_C = \dot{Q}_{Ce} + \dot{Q}_f \tag{16}$$

The power and efficiency of the ESE heat engine operated in intermediate operation regime are

$$P_i = \dot{Q}_H - \dot{Q}_C = \frac{2}{h}\int_{E_R-\Delta E/2}^{E_R+\Delta E/2} (\mu_C - \mu_H)(f_H - f_C) dE \tag{17}$$

$$\eta_i = (\dot{Q}_H - \dot{Q}_C)/\dot{Q}_H = 1 - \dot{Q}_C/\dot{Q}_H \tag{18}$$

It can be seen from equation (17) that the power output P_i is independent of k_f and the filter heat conduction will not affect the power output P_i performance of the ESE heat engine in intermediate operation regime.

Similarly, a numerical example is provided to show the characteristic of the ESE heat engine in intermediate operation regime with given temperatures and potential energy, i.e. $T_H = 2K$, $T_C = 1K$, $\mu_C/k = 12K$ and $\mu_H/k = 10K$.

Figure 6 shows the influence of the temperature of hot reservoir T_H on the power output P_i versus central energy E_R characteristic in intermediate operation regime. It can be seen that the characteristic curves of $P_i - E_R/k_B$ are parabolic like ones. There exists the optimum central energy $(E_R/k_B)_{P_i}$ which leads to the maximum power output $P_{i,max}$. The maximum power output $P_{i,max}$ increases while optimum central energy $(E_R/k_B)_{P_i}$ decrease as the temperature of hot reservoir T_H increases.

Figure 7 shows the influence of the temperature of hot reservoir T_H on the efficiency η_i versus central energy E_R characteristic in intermediate operation regime with $k_f = 1.5\times10^{-14} W/K$ and $E_R/k_B = 2.0K$. It can be seen that the characteristic curves of $\eta_i - E_R/k_B$ with filter heat conduction are also parabolic like ones. There exists the optimum central energy $(E_R/k_B)_{\eta_i}$ which leads to the maximum efficiency $h_{i,max}$. The maximum efficiency $h_{i,max}$ increases and the optimum central energy $(E_R/k_B)_{\eta_i}$ decreases as the temperature of hot reservoir T_H increases.

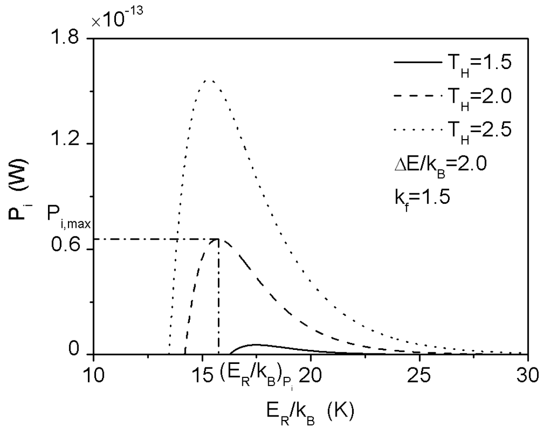

Figure 6. Influence of the temperature of hot reservoir T_H on the power output P_i versus central energy E_R characteristic in intermediate operation regime with $k_f = 1.5\times10^{-14} W/K$ and $\Delta E/k_B = 2.0K$

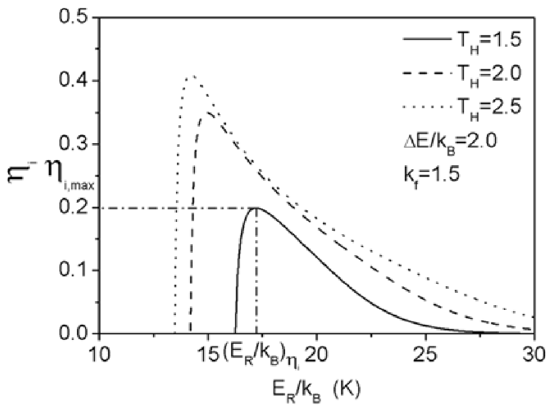

Figure 7. Influence of the temperature of hot reservoir T_H on the efficiency η_i versus central energy E_R characteristic in intermediate operation regime with $k_f = 1.5\times10^{-14} W/K$ and $\Delta E/k_B = 2.0K$

The influence of resonance width ΔE on the power output P_i versus central energy E_R characteristic is shown in Figure 8. One can see from Figure 8 that both the maximum power output $P_{i,max}$ and its corresponding optimum central energy $(E_R/k_B)_{P_i}$ will increase with the increase of resonance width ΔE.

As the central energy E_R decreases and approaches the special energy E_0 ($E_0/k_B = (T_H\mu_C - T_C\mu_H)/(k_BT_H - k_BT_C) = 14$), the power output decreases and becomes negative. This is because only in the energy range of $E_0 < E_R < \infty$, electrons contribute positively to the power output of the heat engine. If $E_R < E_0$, the electron engine system will behave as a refrigerator.

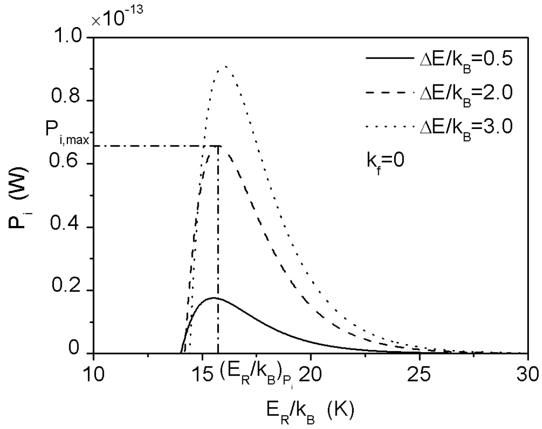

Figure 8. Influence of resonance width ΔE on the power output P_i versus central energy E_R characteristic

Figure 9 and Figure 10 show the influence of resonance width ΔE on the efficiency η_i versus central energy E_R characteristic for given thermal conductivity k_f. It can be seen that the characteristic curves of $\eta_i - E_R/k_B$ with ($k_f \neq 0$) or without ($k_f = 0$) filter heat conduction are all parabolic like ones. When $k_f = 0$, the maximum efficiency $\eta_{i,max}$ decreases and the optimum central energy $(E_R/k_B)_{\eta_i}$ increases as the resonance width ΔE increases. When $k_f \neq 0$, the maximum efficiency $\eta_{i,max}$ first increases and then decreases while the optimum central energy $(E_R/k_B)_{\eta_i}$ increases as the resonance width ΔE increases.

Especially, the characteristic curves of power output P_i versus efficiency η_i in intermediate operation regime are shown in Figure 11 and Figure 12. It can be seen that the characteristic curves of P_i versus η_i are all loop-shaped ones. There exist the optimum efficiency η_{i,P_i} corresponding to the maximum power output $P_{i,max}$ as well as the optimum power output P_{i,η_i} corresponding to the maximum efficiency $\eta_{i,max}$. Thus, in the intermediate power output operation regime, the optimal regions of the efficiency of the ESE heat engine should be

$$\eta_{i,P_i} \le \eta_i \le \eta_{i,max} \tag{19}$$

where η_{i,P_i} and $\eta_{i,max}$ are two important parameters that determine the lower and upper bounds of the optimum efficiency. The optimal operating regions of the power output should be

$$P_{i,\eta_i} \le P_i \le P_{i,max} \tag{20}$$

where P_{i,η_i} and $P_{i,max}$ are two important parameters that determine the lower and upper bounds of the optimum power output. And the optimum regions of the central energy E_R should be

$$(E_R/k_B)_{\eta_i} \le (E_R/k_B) \le (E_R/k_B)_{P_i} \tag{21}$$

Figure 13 shows the influence of heat conductivity k_f on the efficiency η_i versus central energy E_R characteristic for given resonance width ΔE. It shows clearly that as the heat conductivity k_f increases, the maximum efficiency $\eta_{i,max}$ will decrease while the optimum central energy $(E_R/k_B)_{\eta_i}$ will increase. Thus, increasing the heat conduction will always reduce the efficiency of the heat engine.

Figure 14 shows the influence of heat conductivity k_f on the power output P_i versus efficiency η_i for the ESE heat engine in intermediate operation regime. The maximum power output $P_{i,max}$ stays unchanged as the heat conductivity k_f increases. The optimum efficiency η_{i,P_i} corresponding to the maximum power output decreases while the optimum power output P_{i,η_i} corresponding to the maximum efficiency increases as k_f increases. It is worth pointing out that the ESE heat engine model with filter heat conduction discussed in this paper is more general than those presented in Refs. [39, 40]. The important results in these references can be directly derived from the special case that $k_f = 0$ in the present paper. Setting $k_f = 0$ in the present analysis, one can get the performance characteristics of the ESE heat engine in the two different operation regimes without considering filter heat conduction, which are just the results obtained in Ref. [39, 40].

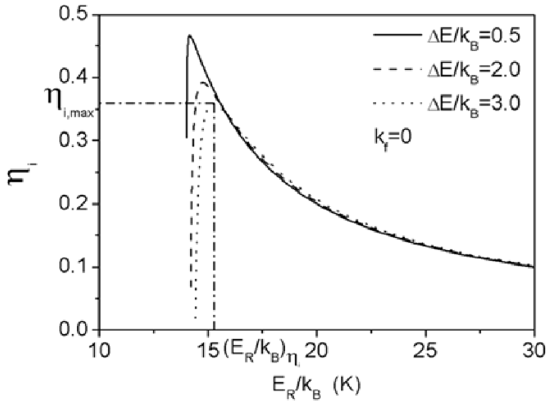

Figure 9. Influence of resonance width ΔE on the efficiency η_i versus central energy E_R characteristic without filter heat conduction ($k_f = 0$)

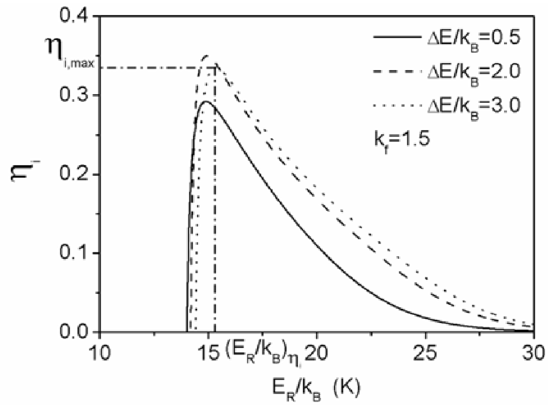

Figure 10. Influence of resonance width ΔE on the efficiency η_i versus central energy E_R characteristic with filter heat conduction ($k_f = 1.5\times10^{-14} W/K$)

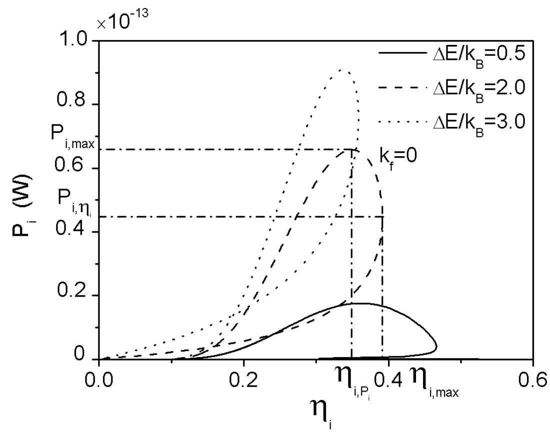

Figure 11. Power output P_i versus efficiency η_i characteristic in intermediate operation regime without filter heat conduction ($k_f = 0$)

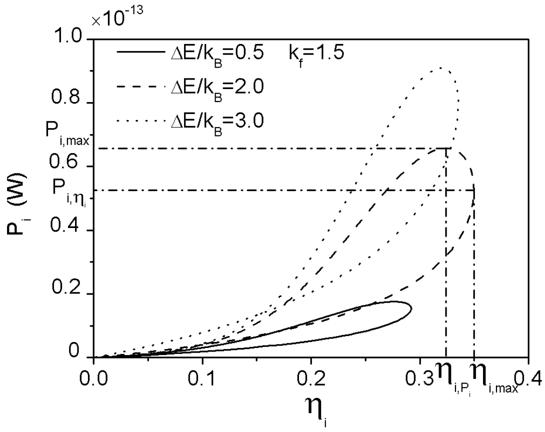

Figure 12. Power output P_i versus efficiency η_i characteristic in intermediate operation regime with filter heat conduction ($k_f = 1.5\times10^{-14} W/K$)

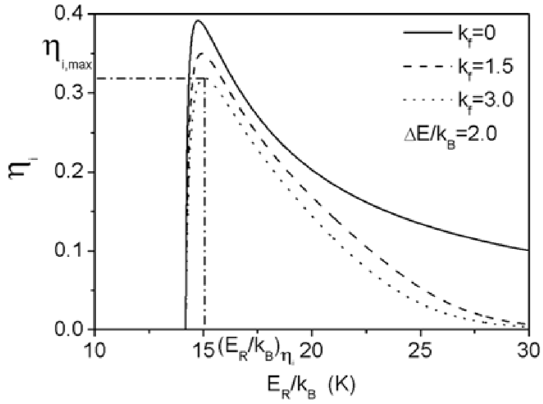

Figure 13. Influence of heat conductivity k_f on the efficiency η_i versus central energy E_R characteristic for given resonance width $\Delta E/k_B = 2.0K$

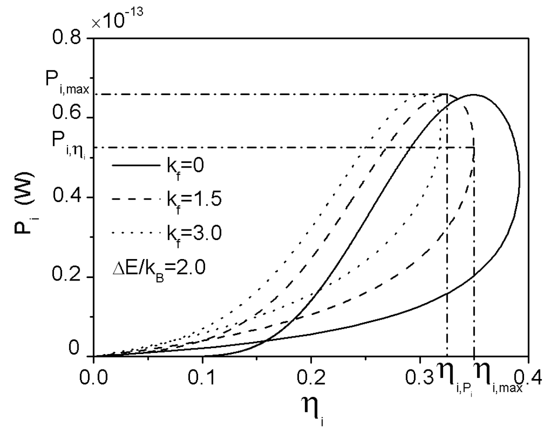

Figure 14. Influence of heat conductivity k_f on the power output P_i versus efficiency η_i characteristic for the ESE heat engine in intermediate operation regime with $\Delta E/k_B = 2.0K$.

5. Conclusions

A model of an energy selective electron (ESE) heat engine with filter heat conduction via the propagation of phonons is proposed in this paper. The general expressions for power output and efficiency of the ESE heat engine are derived for the maximum power operation regime and the intermediate operation regime, respectively. The optimum performance and the optimal operation regions in the two different operation regimes of the ESE heat engine are analyzed by detailed numerical calculations. Results of numerical calculations show that, in maximum power operation regime, due to the existence of energy filter heat conduction, the power versus efficiency characteristic curve changes from parabolic-like one (without filter heat conduction) to a loop-shaped one (with filter heat conduction), and the optimum regions of power output and efficiency should be P_{m,h_m} £ P_m £ $P_{m,max}$ and $\eta_{m,P_m} \le \eta_m \le \eta_{m,max}$. While in intermediate operation regime, the power versus efficiency characteristic curves are always loop-shaped ones and the heat conduction of the filter does not change the shape of characteristic curves. The optimum regions of power output and efficiency in intermediate regime should be P_{i,h_i} £ P_i £ $P_{i,max}$ and $\eta_{i,P_i} \le \eta_i \le \eta_{i,max}$. The influences of filter heat conduction and the temperature of hot reservoir on the performance of the ESE heat engine are also analyzed. It is shown that, in both operation regimes, the power output will not be affected while the efficiency will be reduced by the filter heat conduction; both power output and efficiency will increase as the temperature of hot reservoir increases. In intermediate operation regime, the resonance width also has significant influence on the performance of the ESE heat engine. The maximum power output will increase as resonance width increases no matter the filter heat conduction is considered or not. The efficiency will decrease as resonance width increases when the filter heat conduction is not considered, but it will first increase and then decrease as resonance width increases when the filter heat conduction is considered. The results obtained herein have theoretical significance for understanding and improving the performance of practical electron energy conversion systems.

Acknowledgements
This paper is supported by The National Natural Science Foundation of P. R. China (Project No. 10905093), Program for New Century Excellent Talents in University of P. R. China (Project No. NCET-04-1006) and The Foundation for the Author of National Excellent Doctoral Dissertation of P. R. China (Project No. 200136).

Nomenclature

E	energy of electrons (J)
eV_0	bias voltage
f	fermi distribution of electrons
g	a defined function
h	Plank constant
k_B	Boltzmann's constant
k_f	thermal conductivity of the filter (W/K)
P	power output (W)
$\dot{q}$	rate of heat transfer over a small energy range δE (W)
$\dot{Q}$	rate of heat transfer (W)
T	temperature (K)
ΔE	resonance width (J)
δE	a narrow energy range (J)

Greek symbols

η	efficiency
μ	chemical potential (J)

Subscripts

C	cold electron reservoir
Ce	cold reservoir
f	filter
H	hot electron reservoir
He	hot reservoir
i	intermediate operation regime
m	maximum power operation regime

References

[1] Hatsopoulos G N, Gyftopoulos E P. Thermionic Energy Conversion-Vol 1: Processes and Devices. Cambridge: MIT Press, 1973.

[2] Mahan G D. Thermionic refrigeration. J. Appl. Phys., 1994, 76(7): 4362-4366.

[3] Shakouri A, Bowers J E. Heterostructure integrated thermionic coolers. Appl. Phys. Lett., 1997, 71(9): 1234-1236.

[4] Mahan G D, Woods L M. Multilayer thermionic refrigeration. Phys. Rev. Lett., 1998, 80(18): 4016-4019.

[5] Shakouri A, LaBounty C, Piprek J, Abraham P, Bowers J E. Thermionic emission cooling in single barrier heterostructures. Appl. Phys. Lett., 1999, 74(1): 88-89.

[6] Vining C B, Mahan G D. The b factor in multilayer thermionic cooling. J. Appl. Phys., 1999, 86(12): 6852-6853.

[7] Ulrich M D, Barnes P A, Vining C B. Comparison of solid-state thermionic refrigeration with thermoelectric refrigeration. J. Appl. Phys., 2001, 90(3): 1625-1631.

[8] Hishinuma Y, Geballe T H, Moyzhes B Y, Kenny T W. Measurement of cooling by room-temperature thermionic emission across a nanometer gap. J. Appl. Phys., 2003, 94(7): 4690-4696.
[9] Humphrey T E, O'Dwyer M F, Linke H. Power optimization in thermionic devices. J. Phys. D: Appl. Phys., 2005, 38(12): 2051-2054.
[10] O'Dwyer M F, Humphrey T E, Lewis R A, Zhang C. Low thermal conductivity short-period super lattice thermionic devices. J. Phys. D: Appl. Phys., 2006, 39(19): 4153-4158.
[11] O'Dwyer M F, Lewis R A, Zhang C. Thermionic refrigerators with non-Richardson current. J. Phys. D: Appl. Phys., 2007, 40(4): 1167-1174.
[12] Astumian R D. Thermodynamics and kinetics of a Brownian motor. Science, 1997, 276(5314): 917-922.
[13] Derényi I, Astumian R D. Efficiency of Brownian heat engines. Phys. Rev. E, 1999, 59(6): 6219-6222.
[14] Hondou T, 1. Sekimoto K. Unattainability of Carnot efficiency in the Brownian heat engine. Phys. Rev. E, 2000, 62(5): 6021-6025.
[15] Reimann P. Brownian motors: Noisy transport far from equilibrium. Phys. Rep., 2002, 361(2/4): 57-265.
[16] Schliwa M, Woehlke G. Molecular motors. Nature, 2003, 422(6933): 759-765.
[17] Van den Broeck C, Kawai R, Meurs P. Microscopic analysis of a thermal Brownian motor. Phys. Rev. Lett., 2004, 93(9): 090601.
[18] Asfaw M, Bekele M. Current, maximum power and optimized efficiency of a Brownian heat engine. Eur. Phys. J. B, 2004, 38(3), 457-461.
[19] Van den Broeck C, Kawai R. Brownian refrigerator. Phys. Rev. Lett., 2006, 96(21): 210601
[20] van den Broek M, Van den Broeck C. Chiral Brownian heat pump. Phys. Rev. Lett., 2008, 100(13): 130601.
[21] Berger F, Schmiedl T, Seifert U. Optimal potentials for temperature ratchets. Phys. Rev. E, 2009, 79(3): 031118.
[22] Hänggi P, Marchesoni F. Artificial Brownian motors: Controlling transport on the nanoscale. Rev. Mod. Phys., 2009, 81(1): 387-442.
[23] Schönborn J B, Herges R, Hartke B. Brownian molecular rotors: Theoretical design principles and predicted realizations. J. Chem. Phys., 2009, 130(23): 234906.
[24] Reimann P, Grifoni M, Hänggi P. Quantum ratchets. Phys. Rev. Lett., 1997, 79(1): 10-12.
[25] Linke H, Humphrey T E, Löfgren A, Sushkov A O, Newbury R, Taylor R P, Omling P. Experimental tunneling ratchets. Science, 1999, 286(5448): 2314-2317.
[26] Yukawa S, Tatara G, Kikuchi M, Matsukawa H. Quantum ratchet. Physica B, 2000, 284-288(2): 1896-1897.
[27] Khrapai V S, Ludwig S, Kotthaus J P, Tranitz H P, Wegscheider W. Double-dot quantum ratchet driven by an independently biased quantum point contact. Phys. Rev. Lett., 2006, 97(17): 176803.
[28] Khrapai V S, Ludwig S, Kotthaus J P, Tranitz H P, Wegscheider W. Counterflow of electrons in two isolated quantum point contacts. Phys. Rev. Lett., 2007, 99(9): 096803.
[29] Hoffmann E A, Linke H. Nanoscale thermometry with a quantum dot. J. Low Temp. Phys., 2009, 154(5/6): 161-171.
[30] Mahan G D, Sofo J O, Bartkowiak M. Multilayer thermionic refrigerator and generator. J. Appl. Phys., 1998, 83(9): 4683-4689.
[31] Astumian R D, Hänggi P. Brownian motors. Phys. Today, 2002, 55(11): 33-39.
[32] Parrondo J M R, de Cisneros B J. Energetics of Brownian motors: A Review. Appl. Phys. A, 2002, 75(2): 179-191.
[33] Linke H, Sheng W, Löfgren A, Xu H, Omling P, Lindelof P E. A quantum dot ratchet: Experiment and theory. Europhys. Lett., 1998, 44(3): 341-347.
[34] Linke H, Sheng W, Löfgren A, Xu H, Omling P, Lindelof P E. Lindelof. Erratum, a quantum dot ratchet: Experiment and theory. Europhys. Lett., 1999, 45(3): 406.
[35] Linke H, Sheng W, Svensson A, Löfgren A, Christensson L, Xu H, Omling P, Lindelof P E. Asymmetric nonlinear conductance of quantum dots with broken inversion symmetry. Phys. Rev. B, 2000, 61(23): 15914-15926.
[36] Humphrey T E, Linke H, Newbury R. Pumping heat with quantum ratchets. Physica E, 2001, 11(2/3): 281-286.

[37] Linke H, Humphrey T E, Lindelof P E, Löfgren A, Newbury R, Omling P, Sushkov A O, Taylor R P, Xu H. Quantum ratchets and quantum heat pumps. Appl. Phys. A, 2002, 75(2): 237-246.
[38] Linke H, Humphrey T E, Taylor R P, Micolich A P, Newbury R. Quantum ratchets act as heat pumps. Physica B, 2002, 314(1/4): 464-468.
[39] Humphrey T E, Newbury R, Taylor R P, Linke H. Reversible quantum Brownian heat engines for electrons. Phys. Rev. Lett., 2002, 89(11): 6801-6803.
[40] Humphrey T E. Mesoscopic Quantum Ratchets and the Thermodynamics of Energy Selective Electron Heat Engines. Ph. D. Thesis, University of New South Wales, Australia, 2003.
[41] Edward H L, Niu Q, de L ozanne A L. A quantum-dot refrigerator. Appl. Phys. Lett., 1993, 63(13): 1815-1817.
[42] Vashaee D, Shakouri A. Electronic and thermoelectric transport in semiconductor and metallic superlattices. J. Appl. Phys., 2004, 95(3): 1233-1245.
[43] Vashaee D, Shakouri A. Improved thermoelectric power factor in metal-based superlattices. Phys. Rev. Lett., 2004, 92(10): 106103.
[44] Fan X, Zeng G, LaBounty C, Bowers J E, Croke E, Ahn C C, Huxtable S, Majumdar A, Shakouri A. SiGeC/Si superlattice microcoolers. Appl. Phys. Lett., 2001, 78(11):1580-1582.
[45] O'Dwyer M F, Lewis R A, Zhang C, Humphrey T E. Electronic efficiency in nanostructured thermionic and thermoelectric devices. Phys. Rev. B, 2005, 72(20): 205330.
[46] Humphrey T E, O'Dwyer M F, Zhang C, Lewis R A. Solid-state thermionics and thermoelectrics in the ballistic transport regime. J. Appl. Phys., 2005, 98(2): 026108.
[47] Humphrey T E, Linke H. Reversible thermoelectric nanomaterials. Phys. Rev. Lett., 2005, 94(9):096601.
[48] O'Dwyer M F, Humphrey T E, Linke H. Concept study for a high-efficiency nanowire based thermoelectric. Nanotechnology, 2006, 17(11): S338- S343.
[49] O'Dwyer M F, Humphrey T E, Lewis R A, Zhang C. Efficiency in nanometer gap vacuum thermionic refrigerators. J. Phys. D: Appl. Phys., 2009, 42(3): 035417.
[50] Andresen B, Berry R S, Ondrechen M J, Salamon P. Thermodynamics for processes in finite time. Acc. Chem. Res., 1984, 17(8): 266-271.
[51] Bejan A. Entropy generation minimization: The new thermodynamics of finite-size devices and finite-time Processes. J. Appl. Phys., 1996, 79(3): 1191-1218.
[52] Berry R S, Kazakov V A, Sieniutycz S, Szwast Z, Tsirlin A M. Thermodynamic Optimization of Finite Time Processes. Chichester: Wiley, 1999.
[53] Chen L, Wu C, Sun F. Finite time thermodynamic optimization of entropy generation minimization of energy systems. J. Non-Equilib. Thermodyn., 1999, 24(4): 327-359.
[54] Wu C, Chen L, Chen J. Recent Advances in Finite Time Thermodynamics. New York: Nova Science Publishers, 1999, p560.
[55] Chen L, Sun F. Advances in Finite Time Thermodynamics: Analysis and Optimization. New York: Nova Science Publishers, 2004, p240.
[56] Chen L. Finite-Time Thermodynamic Analysis of Irreversible Processes and Cycles. Higher Education Press, Beijing, 2005, p.280.
[57] Muschik W, Hoffmann K H. Endoreversible thermodynamics: A tool for simulating and comparing processes of discrete systems. J. Non-Equilib. Thermodyn., 2006, 31(3): 293-317.
[58] Feidt M. Optimal use of energy systems and processes. Int. J. Exergy, 2008, 5(5/6): 500-531.
[59] Sieniutycz S, Jezowski J. Energy Optimization in Process Systems. Elsevier, Oxford, UK, 2009.
[60] Velasco S, Roco J M M, Medina A, Calvo Hernández A. Feynman's ratchet optimization: Maximum power and maximum efficiency regimes. J. Phys. D: Appl. Phys., 2001, 34 (6): 1000-1006.
[61] Ai B Q, Xie H Z, Wen D H, Liu X M, Liu L G. Heat flow and efficiency in a microscopic engine. Eur. Phys. J. B, 2005, 48(1): 101-106.
[62] Zhang Y, Lin B, Chen J. Performance characteristics of an irreversible thermally driven Brownian microscopic heat engine. Eur. Phys. J. B, 2006, 53(4): 481-485.
[63] Ai B Q, Wang L, Liu L G. Brownian micro-engines and refrigerators in a spatially periodic temperature field: Heat flow and performances. Phys. Lett. A, 2006, 352(4/5): 286-290.
[64] Schmiedl T, Seifert U. Efficiency at maximum power: An analytically solvable model for stochastic heat engines. Europhys. Lett., 2008, 81(2): 20003.

[65] Tu Z C. Efficiency at maximum power of Feynman's ratchet as a heat engine. J. Phys. A: Math. Theor., 2008, 41(31): 312003.
[66] Lin B, Chen J. Performance characteristics and parametric optimum criteria of a Brownian micro-refrigerator in a spatially periodic temperature field. J. Phys. A: Math. Theor., 2009, 42(7): 075006.
[67] Schmiedl T, Seifert U. Efficiency of molecular motors at maximum power. Europhys. Lett., 2008, 83(3): 30005.
[68] Esposito M, Lindenberg K, Van den Broeck C. Thermoelectric efficiency at maximum power in a quantum dot. Europhys. Lett., 2009, 85(6): 60010.
[69] Esposito M, Kawai R, Lindenberg K, Van den Broeck C. Finite-time thermodynamics for a single-level quantum dot. Europhys. Lett., 2010, 89(2): 20003.
[70] Curzon F L, Ahlborn B. Efficiency of a Carnot engine at maximum power output. Am. J. Phys., 1975, 43(1): 22-24.
[71] Chen G, Shakouri A. Heat transfer in nanostructures for solid-state energy conversion. ASME J. Heat Transfer, 2002, 124(2): 242-252.
[72] Huxtable S T, Abramson A R, Tien CL, Majumdar A, LaBounty C, Fan X, Zeng G, Bowers J E, Shakouri A, Croke E T. Thermal conductivity of Si/SiGe and SiGe/SiGe superlattices. Appl. Phys. Lett., 2002, 80(10):1737-1739.
[73] Kim W, Singer S L, Majumdar A, Vashaee D, Bian Z, Shakouri A, Zeng G and Bowers J E, Zide J M O, Gossard A C. Cross-plane lattice and electronic thermal conductivities of ErAs: InGaAs/ InGaAlAs superlattices. Appl. Phys. Lett., 2006, 88(24): 242107.
[74] He J Z, Wang X M , Liang H N. Optimum performance analysis of an energy selective electron refrigerator affected by heat leaks. Phys. Scr., 2009, 80(3): 035701.
[75] Ding Z, Chen L, Sun F. Performance characteristic of energy selective electron (ESE) refrigerator with filter heat conduction. Rev. Mex. Fis., 2010, 56(2): 125-131.
[76] Bejan A. Theory of heat transfer-irreversible power plant. Int. J. Heat Mass Transfer, 1988, 31(6): 1211-1219.

Zemin Ding received his BS degree from the Naval University of Engineering, P R China in 2006. He is pursuing for his PhD in power engineering and engineering thermophysics from Naval University of Engineering, P R China. His work covers topics in finite time thermodynamics and technology support for propulsion plants. He is the author or co-author of over 10 peer-refereed papers (eight in English).

Lingen Chen received all his degrees (BS, 1983; MS, 1986, PhD, 1998) in power engineering and engineering thermophysics from the Naval University of Engineering, P R China. His work covers a diversity of topics in engineering thermodynamics, constructal theory, turbomachinery, reliability engineering, and technology support for propulsion plants. He has been the Director of the Department of Nuclear Energy Science and Engineering, the Director of the Department of Power Engineering and the Superintendent of the Postgraduate School. Now, he is the Dean of the College of Naval Architecture and Power, Naval University of Engineering, P R China. Professor Chen is the author or co-author of over 1100 peer-refereed articles (over 490 in English journals) and nine books (two in English).
E-mail address: lgchenna@yahoo.com; lingenchen@hotmail.com, Fax: 0086-27-83638709 Tel: 0086-27-83615046

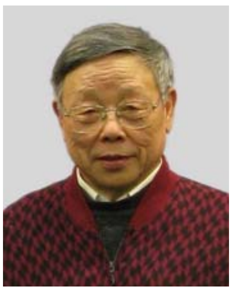

Fengrui Sun received his BS degree in 1958 in Power Engineering from the Harbing University of Technology, P R China. His work covers a diversity of topics in engineering thermodynamics, constructal theory, reliability engineering, and marine nuclear reactor engineering. He is a Professor in the Department of Power Engineering, Naval University of Engineering, P R China. Professor Sun is the author or co-author of over 750 peer-refereed papers (over 340 in English) and two books (one in English).

